Electrical double layer forces. A Monte Carlo study

Lars Guldbrand, Bo Jönsson, Håkan Wennerström, and Per Linse

Citation: The Journal of Chemical Physics **80**, 2221 (1984); doi: 10.1063/1.446912
View online: http://dx.doi.org/10.1063/1.446912
View Table of Contents: http://scitation.aip.org/content/aip/journal/jcp/80/5?ver=pdfcov
Published by the AIP Publishing

Electrical double layer forces. A Monte Carlo study

Lars Guldbrand
Department of Physical Chemistry, Arrhenius Laboratory, S-106 91 Stockholm, Sweden

Bo Jönsson
Division of Physical Chemistry 2, Chemical Center, P. O. Box 740, S-220 07 Lund 7, Sweden

Håkan Wennerström and Per Linse
Division of Physical Chemistry 1, Chemical Center, P. O. Box 740, S-220 07 Lund, Sweden

(Received 20 October 1983; accepted 17 November 1983)

Using a novel method the force between two charged surfaces with an intervening electrolyte solution has been determined from Monte Carlo simulations. We find large deviations from the standard Poisson–Boltzmann treatment of the so called double layer force for divalent counterions at high surface charge densities and at short separations. The deviations have two causes: (i) Due to the inclusion of the effect of ion–ion correlations the counterions concentrate more towards the charged wall reducing the overlap between the double layers; and (ii) correlated fluctuations in the ion clouds of the two surfaces lead to an attractive interaction of a van der Waals type. For some realistic values of the parameters the attraction overcomes the repulsive part and there is a net attractive force between similarly charged surfaces. This finding leads to a modification of our conceptual understanding of the interaction between charged particles and it shows that the DLVO theory is qualitatively deficient under some, realistic, conditions.

I. INTRODUCTION

In colloidal systems electrostatic forces often play a dominant role in determining the physico-chemical properties. This applies to as diverse systems as solutions of charged polymers and latex particles, to biological membranes, lyotropic liquid crystals and micellar solutions, and also to sols and clays. Due to the practical importance of these systems the electrostatic interactions have been extensively studied, and they are considered as one of the central problems in colloidal chemistry. For example, the celebrated DLVO theory[1] has as one of its cornerstones a treatment of the electrostatic double layer interaction based on the Poisson–Boltzmann (PB) approximation.

It is clear from the ability of the DLVO theory to describe the behavior of real colloidal systems[2,3] that the simplifications introduced in the theory are in many cases justified. However, it is also clear that colloidal systems show a complexity and richness in their behavior that calls for attempts to go beyond the DLVO theory in order to obtain a more complete understanding. Such refinements can involve the underlying physical model used in the theory but also improvements of the theoretical treatment of the model. The present article is devoted to a development along the latter line.

The mean field approximation of the Poisson–Boltzmann equation has been analyzed through both more refined analytical approximations[4] and through computer simulations.[5–9] In a series of papers[6,10–13] we have investigated various aspects of the accuracy of the PB approximation in the description of the electrical double layer associated with charged surfaces and particles using the Monte Carlo technique. It has, for example, been shown that the main features of the charge distribution outside a highly charged surface is surprisingly accurately described by the PB equation.

Properties such as the energy and the ion concentration are easily obtained from a Monte Carlo simulation. However, it is technically more problematic to determine the free energy and its derivatives. The colloidal particle–particle interaction is related to an osmotic pressure and it is thus connected to a free energy derivative. In a previous article[11] it was shown that, within the cell model, the osmotic pressure could be obtained from the ion concentration at the cell boundary, in a way analogous to the method used for the PB equation.[14] Here we use this method to investigate more fully the deficiencies in the PB approximation particularly for systems with divalent ions. The method is furthermore extended to incorporate effects due to correlations between two double layers. These give rise to an attractive, van der Waals type force. Such a force has been discussed in connection with polyelectrolyte–polyelectrolyte interactions,[15,16] but it has received little attention in the discussion of colloidal stability. A perhaps surprising result of the analysis is that the electrical double layer interaction between two similarly charged surfaces can be attractive rather than repulsive!

II. THE MODEL SYSTEMS

The majority of the simulations were performed for model systems of infinite, planar, uniformly charged walls, but some studies have also been made on the interaction between charged spheres. These two geometries are the ones for which the DLVO theory was originally developed.

For the planar case, parameters have been chosen so as to model lamellar liquid crystals formed by ionic amphiphiles [see Fig. 1(a)] but the calculations clearly have implications for a number of other systems. The results can for instance be applied to forces in soap films and clays, between biological membranes, and between mica surfaces. The sol-

 0021-9606/84/052221-08$02.10

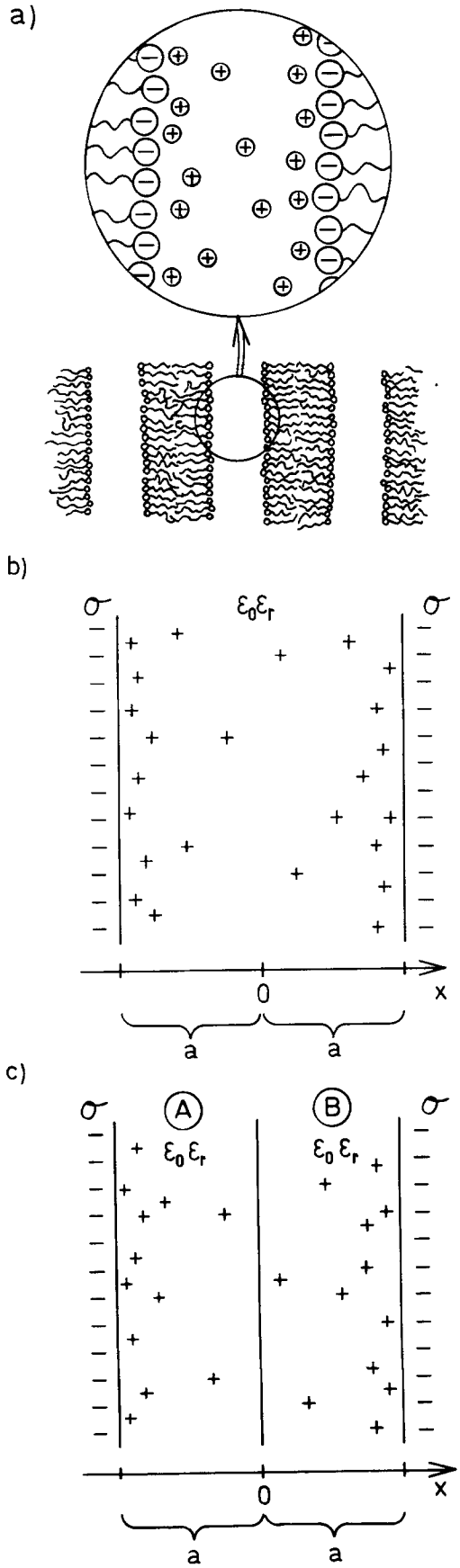

Fig. 1. (a) A schematic representation of a lamellar liquid crystal formed from ionic amphiphiles. (b) A model system for the liquid crystal with planar parallel surfaces of uniform surface charge density σ a distance $2a$ apart. (c) Modified model system with a hard wall in the midplane used for the calculation of the force.

vent (water) is treated as a dielectric continuum, and, at this stage of the investigation, only point charge counterions are present in the solution.

The spherical systems are modeled as micelles formed by charged amphiphiles. The cell model[11] is used and the micelle is represented as a rigid sphere of radius R_b with a uniform charge density σ. The micelle is placed at the center of a spherical cell of radius R_c. The ions in the region between R_b and R_c are either counterions only or both counterions and coions with radius R_a.

In all cases the aggregates themselves have the same relative permittivity as the medium. This means that image charge effects are neglected in the model, which might involve a serious simplification when results of the calculations are compared to results from experiments on real systems.

III. EVALUATION OF THE OSMOTIC PRESSURE

For the discussion of colloidal stability and particle–particle interactions one is interested in the force–distance relation between particles. For infinite planar surfaces, and for particles large enough that the effect of curvature can be neglected, the force can be obtained directly from the osmotic pressure of the model system in Fig. 1(b), provided that the osmotic pressure of a reference (bulk) system is known. For the spherical system the use of the cell model makes the osmotic pressure only indirectly related to interparticle interactions. The model is probably best applied when the spherical particle is symmetrically surrounded by neighbors as in an ordered latex particle system[17] or in a cubic liquid crystal[18] built from spherical aggregates.

In the PB approximation the osmotic pressure is determined by the total ion concentration at the surface of zero electrical field.[14] In the cell model this relation holds strictly and the osmotic pressure is

$$p_{\text{osm}} = kT\sum_i C_i(R_c), \tag{1}$$

where $C_i(R_c)$ is the concentration of ion i at the cell boundary. We use this expression for evaluating p_{osm} in the micellar system.

To evaluate p_{osm} for the planar system we used the simplification of one charged and one uncharged wall in Refs. 13 and 14. In such a case an expression like Eq. (1) can be applied directly. For two similarly charged walls one has instead

$$p_{\text{osm}} = kT\sum_i C_i(a) - \sigma^2/(2\epsilon_r\epsilon_0), \tag{2}$$

where $C_i(a)$ is the ion concentration at a charged wall. It is difficult to use Eq. (2) to evaluate p_{osm} from simulations since the right-hand side tends to involve the difference between nearly equal large quantities resulting in a limited numerical accuracy in p_{osm}.

To solve the problem of determining p_{osm} for the lamellar system with two interacting double layers we have introduced a slightly modified system. The total system is partitioned into two separate but interacting subsystems by introducing a hard wall in the midplane between the two

charged surfaces [see Fig. 1(c)]. The hard wall prevents ions from moving from one half to the other, but it is transparent to electrical interactions. The configurational integral Z_{2N} for the total $2N$ particle system is

$$Z_{2N} = \int_A \int_B \exp[-(U_{AA} + U_{BB} + U_{AB})/kT]\, d\mathbf{r}_A^N\, d\mathbf{r}_B^N, \quad (3)$$

where U_{AA} and U_{BB} represents interactions within the two subsystems A and B, respectively. The interactions between the systems are contained in U_{AB}. When the distance between the two charged walls is changed, Z_{2N} is affected through two mechanisms. To get a clear conceptual picture of the process, make a small increase in the separation in two steps. First the two subsystems are separated a distance Δx, so that a gap is created in the middle. Z_{2N} is then changed only through the interaction term U_{AB}, and the free energy derivative of this process is

$$-\frac{\partial A}{\partial x} = kT\frac{\partial \ln Z_{2N}}{\partial x} = \frac{-1}{Z_{2N}}\int_A\int_B \frac{\partial U_{AB}}{\partial x} \times \exp[-(U_{AA} + U_{BB} + U_{AB})/kT] \times d\mathbf{r}_A^N\, d\mathbf{r}_B^N = F_x^{AB}, \quad (4)$$

where F_x^{AB} is the average force between the two subsystems. In the next step the hard walls at the center are moved $\Delta x/2$ each so that they coincide again. For this process Eq. (1) applies and the total osmotic pressure for the lamellar system is obtained from

$$p_{osm} = kT\sum C_i(0) + F_x^{AB}/\text{area}, \quad (5)$$

where $C_i(0)$ is the ion concentration at the midplane. In contrast to Eq. (2) p_{osm} can be evaluated with satisfactory numerical accuracy from Eq. (5). The modification of the system with the central hard wall is not a serious complication, since in the thermodynamic limit the systems with and without the hard wall have the same properties. In the simulations it is sufficient to ensure that the systems are made large enough so that p_{osm} has converged to the macroscopic value.

Yet another way of calculating p_{osm} is to determine the Helmholtz free energy A (see Sec. V) at different separations of the charged walls. The derivative $\partial A/\partial x$ giving p_{osm} is then obtained numerically. This procedure is very time consuming and it is difficult to achieve a satisfactory precision. In Table I we show a comparison between the different methods of calculating p_{osm} for a couple of cases. The three methods agree within the error limits but it is apparent that only the method based on Eq. (5) is numerically satisfactory.

TABLE I. Comparison between three different methods of obtaining the osmotic pressure for a planar system. $\sigma_0 = 0.2244$ C·m^{-2}.

z	$2a$, Å	σ	p_{osm}/RT, mM		
			from Eq. (5)	from Eq. (2)	from Fig. 7
1	12	σ_0	993 ± 60	700 ± 300	700 ± 400
1	21	σ_0	388 ± 40	600 ± 300	
1	21	$\sigma_0/10$	164 ± 10	149 ± 7	
1	21	$\sigma_0/100$	95 ± 4	91 ± 5	
2	12	σ_0	-127 ± 20	-300 ± 500	-200 ± 500
2	21	σ_0	2 ± 9	-400 ± 500	
2	21	$\sigma_0/10$	46 ± 5	43 ± 10	
2	21	$\sigma_0/100$	10.0 ± 0.3	10.2 ± 0.5	

IV. MONTE CARLO SIMULATIONS

The Monte Carlo (MC) simulations were performed in the canonical ensemble essentially as described previously.[6,13] For the planar system the MC box was a prism with one dimension determined by the separation $2a$ between the charged surfaces, while the extension of the box in the lateral directions follows from the surface charge density σ, the counterion charge ze, and the number of counterions $2N$. The minimum image technique was used and corrections for long range electrostatic forces were made using the PB solution.[6,13] For system sizes larger than about 50 ions no significant changes occurred on further enlargement of the system. In most simulations reported below a system size of 80 ions has been used. The system seems to be well equilibrated after about 2000 configurations per particle and the analysis was then made during at least an additional 2000 configurations per particle.

The electrostatic energy E_{tot} for the whole system can be divided into

$$E_{tot} = E_{ii} + E_{iW} + E_{iPB} + E_{WW} + E_{WPB}. \quad (6)$$

Here, E_{ii} is the energy of interaction between the mobile ions, E_{iW} the ion–wall energy, E_{iPB} the energy due to interactions of ions in the MC box with the (mean field) charge distribution outside the box, E_{WW} is the wall–wall interactions, and finally E_{WPB} the interaction energy due to the charged wall in the box and the charge distribution outside the box. The last two terms are independent of the configuration.

The force F_x^{AB} in the x direction is obtained in a way analogous to the energy and

$$F_x^{AB} = F_{ii} + F_{iW} + F_{Wi} + F_{iPB} + F_{WW} + F_{WPB}. \quad (7)$$

For a particular configuration the ion–ion force is

$$F_{ii} = \frac{z^2e^2}{4\pi\epsilon_r\epsilon_0}\sum_m^A \sum_n^B \Delta x_{mn}/r_{mn}^3, \quad (8)$$

where Δx is the separation in the x direction and r the distance between the ions. The ion–wall term is obtained through integration [cf. Eq. (16) of Ref. 6]

$$F_{iW} = \frac{ze\sigma}{2\pi\epsilon_r\epsilon_0}\sum_m^A \left\{\arcsin\left(\frac{b^4 - x_m^4 - 2b^2x_m^2}{(b^2 + x_m^2)^2}\right) + \pi/2\right\} \quad (9)$$

with an analogous expression for the wall–ion term. On average $F_{iW} = F_{Wi}$. The forces due to the long range correction F_{iPB} for each x value is obtained by a numerical integration of the PB solution and the result is stored in a table. The two last terms in Eq. (7) are again independent of the configuration and can be calculated once for each simulation.

V. RESULTS

The simulations have been performed with both monovalent and divalent counterions. The dielectric properties of the medium were chosen to mimic those of water around

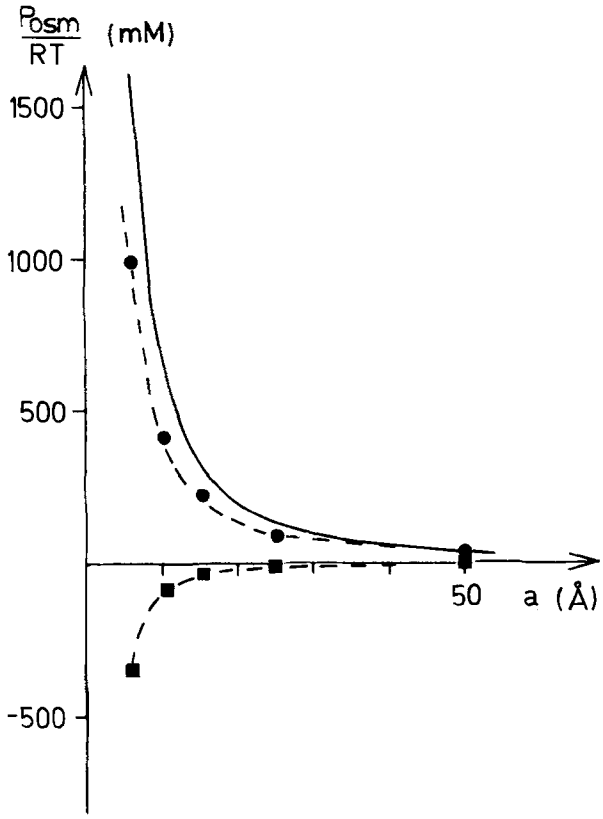

FIG. 2. The osmotic pressure as a function of the distance $2a$ between the charged surfaces for the lamellar system with monovalent counterions. The solid curve is the PB results, while the symbols represent the MC values of the total pressure (●) and the attractive term F_x^{AB}/area(■). $\sigma = 0.2244$ C m^{-2}.

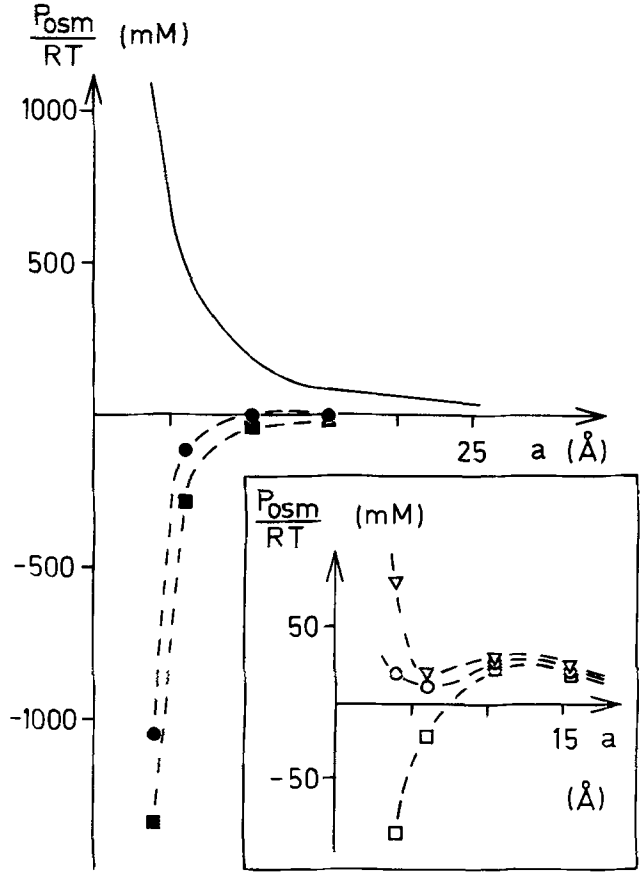

FIG. 3. As in Fig. 2 but for divalent ions. The insert shows MC results for a series of lower σ values: $\sigma = 0.09$ C m^{-2} (□), $\sigma = 0.08$ C m^{-2} (○), and $\sigma = 0.07$ C m^{-2} (▽).

room temperature so that $\epsilon, T = 2.327 \times 10^4$K. Series of simulations have been performed with systematic variations of the different parameters to investigate the general behavior of the system.

For the lamellar case the distance between the charged walls was varied between 8 and 100 Å for a charge density $\sigma = 0.2244$ C m^{-2} corresponding to one unit charge per 71.4 Å^2, which is a typical value for lamellar liquid crystals.[18] For monovalent ions the variation in distance corresponds to a variation from 5.8 to 0.47 M in the mean ion concentration. The calculated osmotic pressure is shown in Figs. 2 and 3 for monovalent and divalent counterions, respectively, and the corresponding PB results are given for comparison. Note that for divalent ions p_{osm} becomes negative at short separations, which means that the surfaces attract one another. To investigate this aspect further the charge density was decreased and as shown in the insert of Fig. 3 the attractive region disappears when $\sigma \lesssim 0.08$ C m^{-2}.

In another series of simulations the surface charge density was varied at a constant separation of 21 Å of the charged surfaces (see Figs. 4 and 5). Figure 5 reveals that also in this case there is an attraction for divalent ions at charge densities higher than $\sigma = 0.20$ C m^{-2}.

The effect of varying the charge density has also been studied for the spherical model system. The radius of the sphere was chosen as $R_b = 30$ Å and the cell radius $R_c = 38$ Å. Figure 6 shows the results for divalent ions, and in this case there is also a study of the effect of an added 1:1 electrolyte on p_{osm}. In the latter simulations the ion radius was chosen to be 1 Å and the micelle radius has thus been reduced to 29 Å.

The excess Helmholtz free energy A^{ex} was determined for the lamellar system at four separations and $\sigma = 0.2244$ C m^{-2} through a charge integration procedure[10]

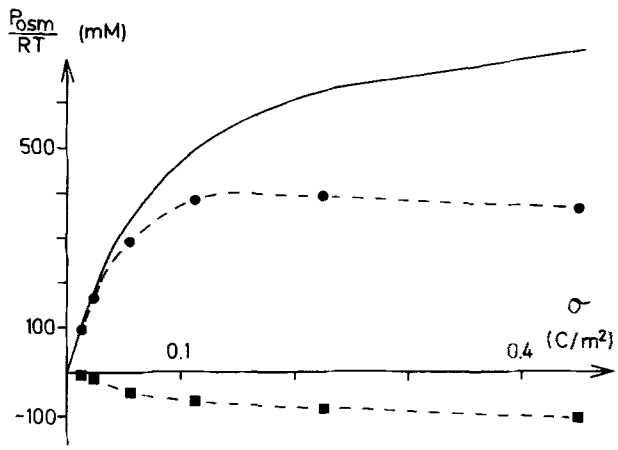

FIG. 4. The osmotic pressure as a function of the surface charge density for monovalent counterions. The distance $2a$ between the walls is 21 Å. Notation as in Fig. 2.

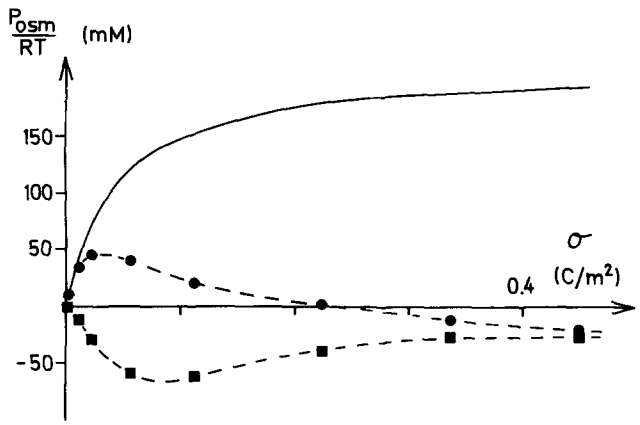

FIG. 5. As in Fig. 4 but for divalent ions.

$$A^{ex} = 2\int_0^1 E_{tot}(\lambda)/\lambda \, d\lambda. \tag{10}$$

Simulations were performed for $\lambda = 0.1, 0.2$—1.0 and the integral was determined numerically. The resulting uncertainty in A^{ex} is due mainly to the statistical uncertainty in E_{tot}. The total free energy is obtained by adding an entropy term for the ideal uncharged system. The resulting free energies are shown in Fig. 7 for both monovalent and divalent ions. For comparison the slope calculated directly through the force is also included in the figure.

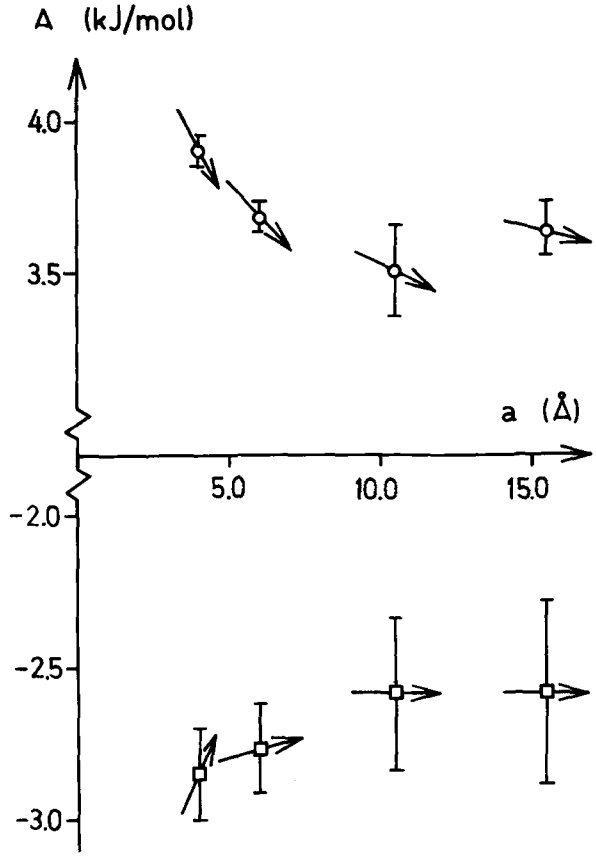

FIG. 7. Calculated Helmholtz free energy for different separations of the charged surfaces in the lamellar system both for monovalent (○) and divalent (□) counterions. For comparison, the arrows indicate the slope expected from the direct evaluation of the osmotic pressure from Eq. 5.

VI. DISCUSSION

A. Contributions to the osmotic pressure

Of the two terms contributing to p_{osm} in Eq. (5) the first one has its origin in the entropy of mixing for the system. A completely analogous term appears in the PB description. It gives necessarily a positive (repulsive) contribution to p_{osm} and is well understood. The mechanisms leading to the second term of the right-hand side of Eq. (5) have received much less attention. It is due to correlated charge fluctuations in the two subsystems and it always leads to a negative (attractive) contribution to p_{osm}. On the average, the electrical field generated by one half of the lamellar system is zero at the position of the other half, but for every configuration there is a spatially varying field. The charges of the second half respond to this instantaneous field and a correlation is developed. In connection with discussions of the DLVO theory this contribution has apparently been largely neglected,[19,20] although a study based on the hypernetted-chain approximation indicates the presence of an attractive term.[21] In the polyelectrolyte field the attraction has received some attention.[15,16] Oosawa has made a qualitative estimate of the importance of the effect and he arrived at the conclusion that for divalent ions a significant attraction term appears, a conclusion that is corroborated by the present work. To our knowledge quantitative values for the attractive force have not been reported previously, and for this reason they are also included in Figs. 2–5.

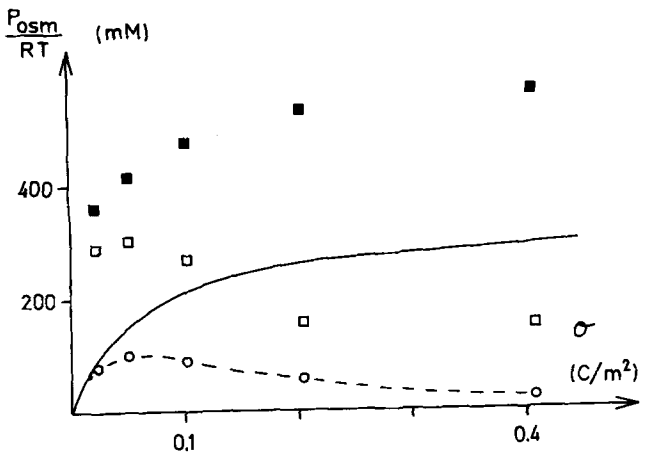

FIG. 6. The osmotic pressure for a micellar system as a function of the charge density σ. The solid curve and the open circles (○) are the PB and MC values without added salt. The addition of a 1:1 electrolyte of 0.128 M with respect to the aqueous region results in higher total pressures both for the PB (■) and MC (□) calculations.

From Fig. 5 it is seen that both terms of Eq. (5) have a maximum at approximately the same value of σ. To trace the origin of this behavior the attractive force was analyzed in more detail for a particular case. The lamellar system was divided into six slices as shown in Fig. 8 and the force

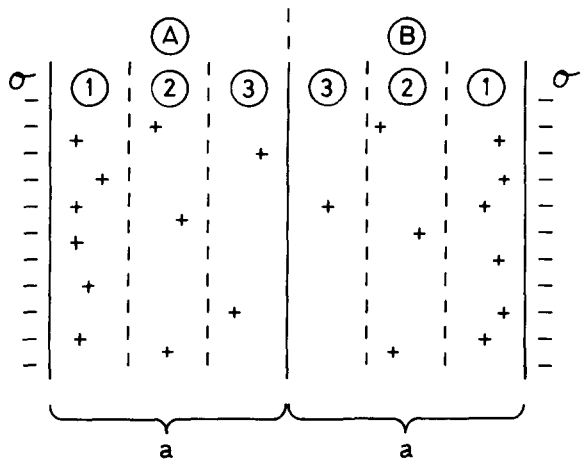

FIG. 8. The modified planar model system subdivided into six layers parallel to the walls. The forces across the midplane from interactions between the different layers are calculated in the simulation to determine where the attraction is predominantly generated.

between the different slices was computed in the simulation. The result is summarized in Table II. Counted per charge, the most important contribution to the force comes from the parts of the subsystem that is closest to the central wall. When σ is increased as in Fig. 5 there is a depletion of ions in the center[13] reducing the repulsive term but also reducing the attractive component as indicated by Table II.

B. Ion–ion correlations and the Poisson–Boltzmann approximation

In the preceding subsection the correlations between the two halves of the lamellar system were discussed. In the PB approximation all ion–ion correlations are neglected,[6] which means that not only is the attractive force between the two subsystems left out but there also appears errors in the ion distribution within the subsystems. We have previously argued that when the ion–ion correlations are properly considered this should lead to a contraction of the ion cloud. The present simulations give yet another illustration of this effect, and it is clear that the correlations are more important for divalent ions than for monovalent ones. Yet another aspect of the ion correlation can be obtained from the free energy calculations. In the PB approximation the entropy (considering the dielectric permittivity as temperature independent) is determined from the (one) particle density only.

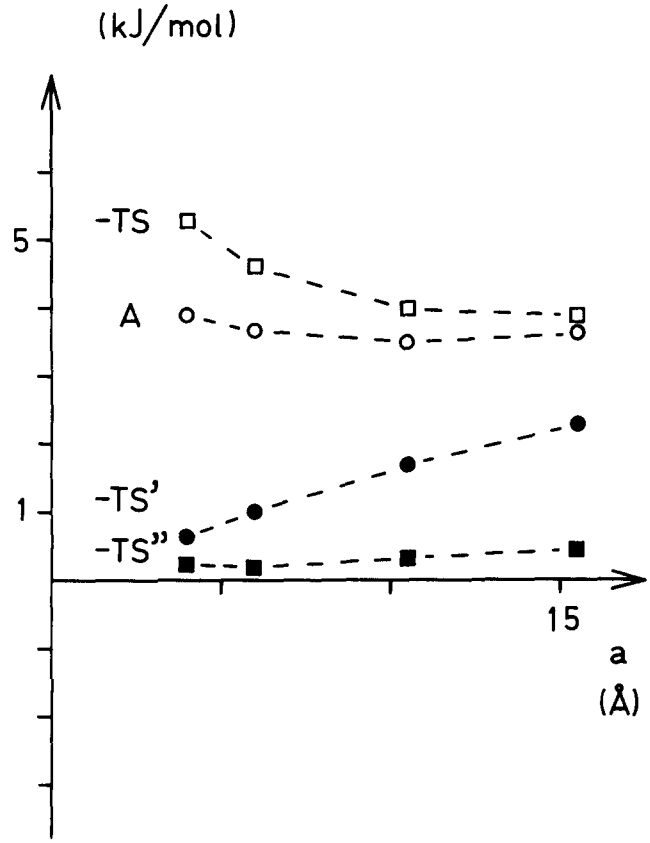

FIG. 9. Different contributions to the Helmholtz free energy A (○) for monovalent counterions and different wall–wall separations. The entropy term -TS' (●) arises from the nonuniformity of the one particle distribution, while -TS" (■) contains the correlation effects. The total entropy term -TS (□) includes an ideal entropy of mixing.

In the simulations, contributions from the particle correlations also appear leading to a decrease in the entropy. The magnitude of the effect is illustrated in Figs. 9 and 10 for monovalent and divalent ions, respectively. As seen the contribution from the one particle density dominates but the correlations become more important for divalent ions (cf. Ref. 10).

The free energy can be determined formally from the logarithm of the configuration integral Z_{2N} [cf. Eq. (4)]. A dimensionless length scale can be introduced by the transformation

$$x' = kT\epsilon_r\epsilon_0 x/z^2e^2$$

TABLE II. The components of the attractive force from the interactions between the ions in the different layers of the subdivided system in Fig. 8 in units of mM. [$f_{ii} = F_{ii}/(\text{area}\cdot RT)$]. The correlation effects are seen in the difference Δf_{ii} between the MC values and the mean field (MF) values using the one particle distributions from the simulations. A measure of the relative importance of the effect counted per charge is given by $\Delta f_{ii}/C_kC_l$, where C_k and C_l are the mean ion concentrations of layers k and l, respectively. The total attractive force term from the simulation is $F_x^{AB}/(\text{area}\cdot RT) = 36.7 \pm 1.5$ mM.

Component	f_{ii}, mM		Δf_{ii}, mM	$\Delta f_{ii}/C_kC_l$, $10^{-3}\cdot M^{-1}$
	MC	MF		
$f(3,3)$	0.70 ± 0.24	2.22	-1.52 ± 0.24	-830 ± 130
$f(2,2)$	14.4 ± 1.2	15.40	-1.0 ± 1.2	-68 ± 78
$f(1,1)$	5973 ± 22	5980.27	-7.3 ± 22	-0.7 ± 2.1
$f(3,2)+f(2,3)$	8.8 ± 1.7	11.74	-2.9 ± 1.7	-550 ± 325
$f(3,1)+f(1,3)$	223 ± 37	232.70	-10 ± 37	-72 ± 270
$f(2,1)+f(1,2)$	604 ± 23	607.60	-3.6 ± 23	-9 ± 57

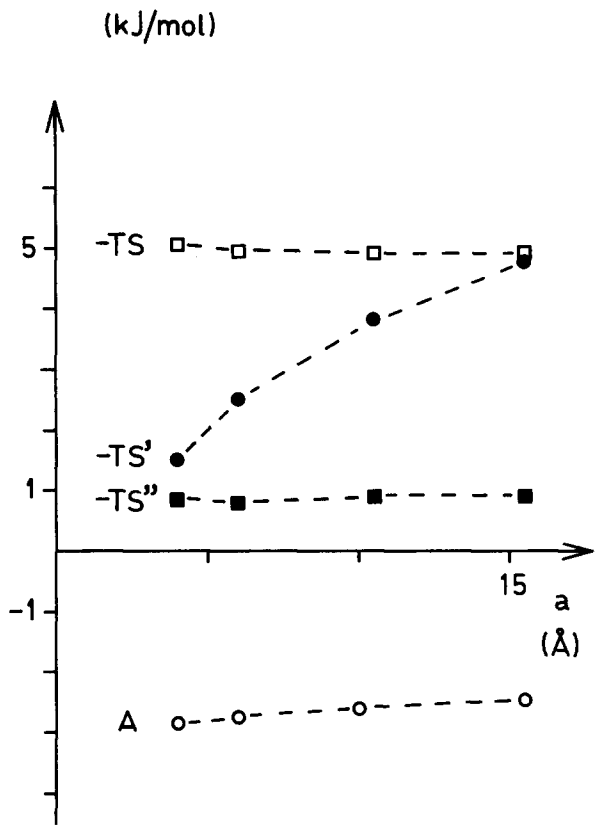

FIG. 10. As in Fig. 9 but for divalent counterions.

for all coordinates. By this transformation Z_{2N} can be seen to be a function of three dimensionless parameters. One of these is the number of particles $2N$ and in the thermodynamic limit

$$Z_{2N} \rightarrow f(S_1,S_2)^{2N}(z^2e^2/kT\epsilon_r\epsilon_0)^{3\cdot 2N}.$$

Z_{2N} is then a function of two parameters S_1 and S_2 only. We chose these as

$$S_1 = kT\epsilon_r\epsilon_0 a/z^2e^2 \tag{11a}$$

$$S_2 = \sigma z^3 e^3/(kT\epsilon_r\epsilon_0)^2. \tag{11b}$$

The corresponding PB solution is determined by one parameter $K = S_1 \cdot S_2$ only.[22]

Correlations become important as the interparticle interactions increase so we expect the largest errors in the PB result to occur for small S_1 and large S_2. The analysis also shows that an increase in the charge ze can be approximately compensated by an increase in $\epsilon_r T$. When we get qualitatively different results for monovalent and divalent ions it should be remembered that this is due to our particular choice of $\epsilon_r T$ and also of the other parameters σ and a.

C. The osmotic pressure

The simulations show that the ion correlations are more crucial in determining the osmotic pressure than in determining the overall ion distribution.[6] Figures 2 and 3 illustrate how p_{osm} varies with the parameter S_1 for a constant S_2. When S_2 is small as in Fig. 2 the PB approximation works reasonably well and (quantitative) discrepancies appear first for small values of S_1 (small separations). If on the other hand S_2 is sufficiently large, there is a qualitative error in the PB treatment and instead of a repulsion there is an attraction for small separations. As shown in the insert in Fig. 3 a systematic lowering of S_2 leads to a gradual transition to the qualitative behavior of Fig. 2. Of particular interest are the results for $\sigma \approx 0.08$ C m^{-2} showing a nonmonotomic change in p_{osm}. In a lamellar system with such a behavior of p_{osm} one expects a phase separation with two lamellar phases with different repeat distances.

In Figs. 4 and 5 the value of S_1 is kept constant and S_2 is varied. Again for small S_2 there is a quantitative agreement with the PB results, while an error develops as S_2 is increased, more dramatically for the smaller value of S_1.

D. Applications

So far the results of the simulations have been compared only to the mean field results of the PB equation. Such a comparison is straightforward since the underlying physical model is one and the same. Comparisons with real physical systems are more problematic due to the uncertainty concerning the applicability of the model. However, the calculations give clear indications on ranges where the DLVO theory is not applicable. For high charge densities, at short separations and for ions of high valency one should clearly apply the PB equation with care in calculations of p_{osm}.

There exists a large body of data on electrostatic forces in colloidal systems to which the present simulations have relevance. Here we limit the discussion to a few particular cases. In several systems of lamellar lyotropic liquid crystals[23,24] it is found that with divalent counterions a concentrated lamellar phase can be in equilibrium with a dilute solution, while under the same conditions the systems with monovalent ions swell extensively. This could be explained by the effects discussed above.

For soap films of the Newton black film type, there is a high surface charge density and a small separation between surfaces. The PB theory is in this case inadequate, which should be one essential reason for the theoretical problems met in explaining the stability of these films.[25] The fact that the Newton black films are formed from systems in equilibrium with a solution of high salt concentration is no serious problem in the application of the results of the simulations since in the actual film there is only a very small amount of coions.

For solutions of charged latex particles there have been preliminary reports of a phase separation between two homogeneous solutions with different concentrations. Such a behavior is indicative of a force–distance relation as in the insert of Fig. 3. The classical electrostatic forces are thus in principle sufficient to induce the phase separation, but a careful quantitative analysis is required to judge which parameters in terms of charge density and particle radius are required for this type of phase separation to occur.

Charged polymers often precipitate in the presence of divalent ions. This is usually interpreted in terms of specific site interactions and bridging processes. As pointed out by Oosawa[15,16] there is the alternative explanation that the behavior is due to an electrostatic attraction instead. A perhaps

more likely explanation is that in the presence of divalent ions the polyion repulsion is reduced to such low values that only very weak specific interactions are required to cause a precipitation.

[1]E. J. W. Verwey and J. Th. G. Overbeek, *Theory of the Stability of Lyophobic Colloids* (Elsevier, Amsterdam, 1948).
[2]D. Eagland, in *Water: A Comprehensive Treatise*, edited by F. Franks (Plenum, New York, 1979), Vol. 5, Chap. 1.
[3]J. N. Israelachvili and G. E. Adams, J. Chem. Soc. Faraday Trans. 1 **74**, 975 (1978).
[4]D. Henderson, Prog. Surf. Sci. **13**, 197 (1983).
[5]G. M. Torrie and J. P. Valleau, Chem. Phys. Lett. **65**, 343 (1979).
[6]B. Jönsson, H. Wennerström, and B. Halle, J. Phys. Chem. **84**, 2179 (1980).
[7]W. Megen and I. Snook, J. Chem. Phys. **73**, 4656 (1980).
[8]G. M. Torrie and J. P. Valleau, J. Phys. Chem. **86**, 3251 (1982).
[9]D. Bratko and V. Vlachy, Chem. Phys. Lett. **90**, 434 (1982).
[10]P. Linse, G. Gunnarsson, and B. Jönsson, J. Phys. Chem. **86**, 413 (1982).
[11]H. Wennerström, B. Jönsson, and P. Linse, J. Chem. Phys. **76**, 4665 (1982).
[12]P. Linse and B. Jönsson, J. Chem. Phys. **78**, 3167 (1983).
[13]B. Jönsson, P. Linse, T. Åkesson, and H. Wennerström, in *Surfactants in Solution*, edited by K. S. Mittal and B. Lindman (Plenum, New York, 1983).
[14]R. A. Marcus, J. Chem. Phys. **23**, 1057 (1955).
[15]F. Oosawa, Biopolymers **6**, 1633 (1968).
[16]F. Oosawa, *Polyelectrolytes* (Dekker, New York, 1971).
[17]S. Hachisu and K. Takano, Adv. Colloid Interface Sci. **16**, 233 (1982).
[18]P. Ekwall, Adv. Liq. Cryst. **1**, 1 (1975).
[19]J. Mahatny and B. W. Ninham, *Dispersion Forces* (Academic, New York, 1976), Chap. 7.
[20]C. J. Barnes and B. Davis, J. Chem. Soc. Faraday Trans. 2 **71**, 1667 (1975).
[21]G. N. Patey, J. Chem. Phys. **72**, 5763 (1980).
[22]S. Engström and H. Wennerström, J. Phys. Chem. **82**, 2711 (1978).
[23]A. Khan, K. Fontell, G. Lindblom, and B. Lindman, J. Phys. Chem. **86**, 4266 (1982).
[24]A. Khan, K. Fontell, and B. Lindman, in *Surfactants in Solution*, edited by K. S. Mittal and B. Lindman (Plenum, New York, 1983).
[25]J. A. de Feijter and A. Vrij, J. Colloid Interface Sci. **70**, 456 (1979).